# Probing spin and orbital Kondo effects with a mesoscopic interferometer

Rosa López and David Sánchez
*Département de Physique Théorique, Université de Genève, CH-1211 Genève 4, Switzerland and Departament de Física, Universitat de les Illes Balears, E-07122 Palma de Mallorca, Spain*

Minchul Lee and Mahn-Soo Choi
*Department of Physics, Korea University, Seoul 136-701, Korea*

Pascal Simon
*Laboratoire de Physique et Modélisation des Milieux Condensés, CNRS et UJF, 38042 Grenoble, France*

Karyn Le Hur
*Département de Physique and RQMP, Université de Sherbrooke, Sherbrooke, Québec, Canada, J1K 2R1*
(Received 16 December 2004; published 18 March 2005)

We investigate theoretically the transport properties of a closed Aharonov-Bohm interferometer containing two quantum dots in the strong coupling regime. We find two distinct physical scenarios depending on the strength of the interdot Coulomb interaction. When the interdot Coulomb interaction is negligible, only spin fluctuations are important and each dot develops a Kondo resonance at the Fermi level independently of the applied magnetic flux. The transport is characterized by the interference of these two independent Kondo resonances. On the contrary, for large interdot interaction, only one electron can be accommodated onto the double-dot system. In this situation, not only the spin can fluctuate but also the orbital degree of freedom (the pseudospin). As a result, we find different ground states depending on the value of the applied flux. When $\phi=\pi \pmod{2\pi}$ ($\phi=2\pi\Phi/\Phi_0$, where $\Phi$ is applied flux and $\Phi_0=h/e$ the flux quantum) the electronic transport can take place via simultaneous correlations in the spin and pseudospin sectors, leading to the highly symmetric SU(4) Kondo state. Nevertheless, we find situations with $\phi>0 \pmod{2\pi}$ where the pseudospin quantum number is not conserved during tunneling events, giving rise to the common SU(2) Kondo state with an enhanced Kondo temperature. We investigate the crossover between both ground states and discuss possible experimental signatures of this physics as a function of the applied magnetic flux.

DOI: 10.1103/PhysRevB.71.115312 PACS number(s): 73.23.−b, 72.15.Qm, 73.63.Kv

## I. INTRODUCTION

Progressive advance in nanofabrication technology has achieved the realization of tiny droplets of electrons termed quantum dots (QDs) with a high-precision tunability of the transport parameters.[1] One of the most exciting features of a QD is its ability to behave as a quantum impurity with spin $1/2$.[2,3] At temperatures lower than the Kondo temperature ($T_K$), the localized spin becomes strongly correlated with the conduction electrons and consequently is screened.[2–4] As a result of the increasing rate of scattering there arises a resonance at the Fermi energy ($E_F$) in the density of states (DOS) of the QD.[4] The transmission through the quantum dot is then almost perfect. This is the so-called *unitary limit* where conductance reaches $2e^2/h$.[5–7] Among many of the advantages offered by QD-based devices, we highlight the possibility of studying the Kondo effect out of equilibrium by applying a dc bias[8] or a time-dependent potential.[9,10]

A natural step forward is the understanding of the magnetic interactions of two artificial Kondo impurities.[11–19] The investigation of double QDs is mainly motivated by the possibility of their application as solid-state quantum bits, by using either spin or charge degrees of freedom.[18–21] When the two QDs are interacting, the orbital degrees of freedom come into play as a pseudospin, as shown experimentally in Refs. 22 and 23, which may give rise to exotic physical scenarios.[24,25] Thus, in a double QD it is possible to tune appropriately the gate voltages in order to find two charge states almost degenerate. If the *inter*dot Coulomb interaction is large enough these two states are $\{n_1=1,n_2=0\}$ and $\{n_1=0,n_2=1\}$, where $n_{1(2)}=\langle\hat{n}_{1(2)}\rangle$ is the charge state in the dot "1" ("2"). This is one of the basic ingredients to observe Kondo physics: the existence of degeneracy between two quantum states. The Kondo effect is then developed to its fullest extent in the pseudospin (orbital) sector. We define the pseudospin $\hat{T}$ as follows: it points along $+(-)z$ when the electron is at the "1" ("2") dot: $\hat{T}^z=(1/2)(\hat{n}_1-\hat{n}_2)$. The pseudospin of the double-QD system can be $1/2$ or $-1/2$, which is quenched (screened) via higher order tunneling processes producing the so-called *orbital Kondo effect*.[22–24] Other realizations of such exotic "orbital Kondo effects" have been recently proposed in different QD-related structures as well.[25–27] When the *intra*dot Coulomb energy for each dot is large, then each QD also behaves as a magnetic impurity and the conventional Kondo effect is also observed in the spin sector ($S^z=\pm 1/2$). The quantum fluctuations between these four states [$S^z=\pm1/2=\{\uparrow,\downarrow\}$ and $T^z=\pm1/2=\{\Uparrow,\Downarrow\}$] lead to an unusual strongly correlated Fermi liquid state in which the (real) spin and pseudospin are totally entangled.[25] In contrast to common spin Kondo physics observed in QDs, this new state possesses a higher symmetry, SU(4), corresponding to

 

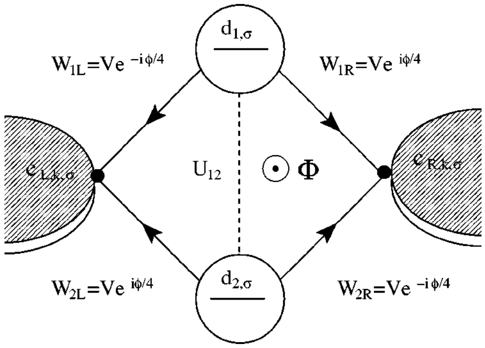


FIG. 1. Sketch of the Aharonov-Bohm interferometer containing two quantum dots attached to two leads. The arrowed straight line indicates the tunnel coupling and the dashed line represents the interdot Coulomb interaction.

the total internal degrees of freedom of the double QD: $\{\uparrow\Uparrow,\downarrow\Uparrow,\uparrow\Downarrow,\downarrow\Downarrow\}$. The screened magnitude is now the *hyperspin* $\hat{M}\equiv\Sigma_{a,b}(\hat{S}^a+1/2)(\hat{T}^b+1/2)$. Importantly, the associated Kondo temperature $T_K^{\mathrm{SU}(4)}$ is much *higher* than in the common spin-1/2 Kondo effect in a QD, which makes the observation of this spin and pseudospin entangled state more accessible.[25] Strong entanglement of charge and spin flip events is also possible in a single-electron box (metallic grain) coupled to a lead via a smaller quantum dot in the Kondo regime.[26,27] Here, the spin Kondo physics stems from the screening of the spin of the small dot, while the pseudospin Kondo physics emerges when charging states of the grain with (charge) $Q=0$ and $Q=e$ are almost degenerate.

The most prominent feature of the Kondo effect is the phase coherence experienced by the electrons that participate in the many-body correlated state. Therefore, it is thus of great interest to have access to the phase of the transmission amplitude in order to give a full characterization of the transport properties. The widely known Aharonov-Bohm (AB) effect[28] provides us a valuable tool to investigate quantum coherence of electrons. When the coherence of a circulating electron wave packet enclosing a magnetic flux $\Phi$ is preserved, the result is an extra flux-dependent phase shift ($\phi$). In the simplest realization of an AB interferometer, an incoming electronic wave function splits into two paths, which join again into the outgoing electronic wave function. Applying a magnetic flux which threads this closed geometry, the outgoing wave function acquires a flux-dependent phase, $\phi=2\pi\Phi/\Phi_0$, where $\Phi=BS$ is the flux, $B$ is the applied magnetic field, $S$ is the enclosing surface, and $\Phi_0=h/e$ the flux quantum. As a consequence, the transmission is a periodic function of $\phi$.

In this work, we consider a double-quantum dot embedded in a prototypical mesoscopic interferometer threading a magnetic flux $\Phi$, see Fig. 1.[29] Our motivation to investigate this system is twofold: (i) there are striking effects, such as Fano resonances, which arise already in the noninteracting case[30–32] and, more interestingly (ii) as the interdot interaction gets stronger, the local density of states on the double QD changes drastically.[33] *Here, we provide a unified picture of the combined influence of wave interference, Kondo effect, and interdot interaction on the electronic transport through a double QD in and out of equilibrium.*

As we anticipated, the physical scenario in our setup will depend much on the strength of the capacitive interdot coupling between the two dots. When the interdot Coulomb energy is negligible, each QD can accommodate one electron and both spins become screened. We find that each QD develops a Kondo resonance at the Fermi level $E_F=0$. Their interference causes a very narrow *dip* in the differential conductance $\mathcal{G}\equiv dI/dV_{\mathrm{dc}}$ except at $\phi\approx 0 \pmod{2\pi}$. In the limit of strong interdot Coulomb interaction there are two degenerate charge states described by the pseudospin $T^z=\pm 1/2$. The presence of flux allows us to explore two interesting situations: (i) when the pseudospin is a good quantum number $[\phi=\pi \pmod{2\pi}]$ and (ii) when the pseudospin is not conserved during tunneling. In the former case the SU(4) Kondo state is fully developed, whereas far away from this symmetry point the conventional SU(2) Kondo physics arises. In addition, we will show that $\mathcal{G}$ shows a zero-bias anomaly (ZBA) instead of a dip when the interdot Coulomb energy is large, which is suppressed as $\phi$ enhances and eventually disappears at the destructive interference condition [when $\phi=\pi \pmod{2\pi}$], resulting in a complete suppression of the tunneling current. Nevertheless, this fact does not prevent us from observing the highly symmetric SU(4) Kondo state since it survives even away from $\phi=\pi \pmod{2\pi}$ where the differential conductance is not totally suppressed.

This work is organized as follows: we begin in Sec. II presenting the theory to treat both limits for the interdot Coulomb interaction using different theoretical techniques. We derive the transport properties as well. In Sec. III we present our numerical results and their interpretation. Finally, we summarize our main conclusions in Sec. IV.

## II. THEORY

The system that we consider is depicted in Fig. 1. It is a closed-geometry AB interferometer, where electrons emitted from the leads are never lost in surrounding gates. Electrons traveling through the device have to go either through the upper dot or through the lower dot before being transmitted into either the left or the right electrode. The area enclosing the two paths is penetrated by a flux $\Phi$. The two reservoirs are Fermi seas of electrons described by the Hamiltonian

$$\mathcal{H}_0=\sum_{\ell=L,R}\sum_{k,\sigma}\varepsilon_{\ell,k}c^{\dagger}_{\ell,k,\sigma}c_{\ell,k,\sigma}, \tag{2.1}$$

where $c^{\dagger}_{L(R),k,\sigma}(c_{L(R),k,\sigma})$ is the creation (annihilation) operator for an electron in the state $k$ with spin $\sigma$ in the lead $L(R)$. The isolated dots are described by $\mathcal{H}_D$

$$\mathcal{H}_{\mathrm{D}}=\sum_{i=1,2}\left[\sum_{\sigma}\varepsilon_i d^{\dagger}_{i,\sigma}d_{i,\sigma}+U_i n_{i,\uparrow}n_{i,\downarrow}\right]+U_{12}n_1n_2. \tag{2.2}$$

The operator $d^{\dagger}_{i,\sigma}(d_{i,\sigma})$ is the creation (annihilation) operator, $\varepsilon_i$ is the level position, $U_i$ are the *intradot* Coulomb interaction, and $n_{i,\sigma}=d^{\dagger}_{i,\sigma}d_{i,\sigma}$ is the occupation number on the dot $i$. $U_{12}$ denotes the *interdot* Coulomb interaction between the dots. The tunneling between the dots and the leads is modeled by $\mathcal{H}_T$

$$\mathcal{H}_T = \sum_{j=1,2}\sum_{\ell=L,R}\sum_{k,\sigma} W_{\ell,j} c^\dagger_{\ell,k,\sigma} d_{j,\sigma} + \text{h.c.} \tag{2.3}$$

The tunneling amplitude $W_{\ell,j}$ in Eq. (2.3) from the dot $j$ to the lead $\ell$ is modulated by the external flux $\Phi$ threading the loop (Fig. 1) and given by

$$W_{L,1} = V_{L,1} e^{-i\phi/4}, \quad W_{L,2} = V_{L,2} e^{+i\phi/4},$$

$$W_{R,1} = V_{R,1} e^{+i\phi/4}, \quad W_{R,2} = V_{R,2} e^{-i\phi/4}, \tag{2.4}$$

where $V_{\ell,j}$ is the amplitude in the absence of the flux and $\phi \equiv 2\pi\Phi/\Phi_0$, with $\Phi_0$ being the flux quantum ($\Phi_0 = h/e$). Then, the total Hamiltonian is $\mathcal{H}_{\text{total}} = \mathcal{H}_0 + \mathcal{H}_D + \mathcal{H}_T$.

To make the physical interpretations of our results more clear, we perform a few simplifications. First of all, we assume identical dots and symmetric junctions; i.e., $\varepsilon_1 = \varepsilon_2 \equiv \varepsilon_d$, $U_1 = U_2 \equiv U$, and $V_{L,1} = V_{L,2} = V_{R,1} = V_{R,2} \equiv V$. This is only for the sake of simplicity.[34] Furthermore, we consider the wide band limit, in which the couplings are independent of energy. Then, the hybridization of the dot levels with the conduction band is well characterized by the parameters

$$\Gamma_{\ell;i,j}(\phi) = \pi\rho_\ell W_{\ell,i} W^*_{\ell,j}, \tag{2.5}$$

or, in the matrix notation

$$\hat{\Gamma}_L(\phi) = \Gamma_L \begin{bmatrix} 1 & e^{-i\phi/2} \\ e^{+i\phi/2} & 1 \end{bmatrix}, \ \hat{\Gamma}_R = \hat{\Gamma}^*_L, \tag{2.6}$$

where $\Gamma_\ell \equiv \pi\rho_\ell V^2$, with $\rho_\ell$ being the DOS in the lead $\ell$ at the Fermi energy ($\rho_L = \rho_R = \rho_0$).

Since we are interested in Kondo correlations,[35] we shall mainly concentrate on the Kondo regime [intradot charging energy $U \to \infty$ and localized level $-\varepsilon_d \gg (\Gamma_L + \Gamma_R)$] for which the fluctuations of the charges in the single dots are highly suppressed. For the interdot Coulomb interaction $U_{12}$, we will investigate two opposite limits, namely (i) $U_{12} = 0$ and (ii) $U_{12} = \infty$. In the former case, each dot is singly occupied ($\langle n_1\rangle = \langle n_2\rangle \approx 1$) and behaves as separate magnetic (Kondo) impurities. In the latter case, the double-quantum dot system contains just one electron ($\langle n_1 + n_2\rangle = 1$). These two limits induce striking differences between the resulting Kondo effects. Moreover, the interference modulated by the external flux $\phi$ threading the AB geometry leads to an even richer variation of the Kondo effects in either case. Our goal is to investigate these scenarios thoroughly. For this purpose we employ different techniques: scaling analysis (valid for $T \gg T_K$), the slave-boson mean-field theory (SBMFT, for $T \ll T_K$), and the numerical renormalization group (NRG) method. We elaborate below on these approaches.

### A. Scaling analysis

We derive effective Hamiltonians in the Kondo regime for the two limiting cases ($U_{12} = 0$ and $U_{12} = \infty$) and discuss their qualitative features at equilibrium by means of the scaling theory.

#### *1. Case* $U_{12} \to 0$

First, we discuss the large capacitance limit between the two dots ($U_{12} \to 0$). As we mentioned, when $U_{12}$ is vanishingly small (and yet $U_1, U_2 \to \infty$), the two dots are both singly occupied: $\langle n_1\rangle = \langle n_2\rangle \approx 1$ and each dot can thus be regarded as a magnetic impurity with spin $1/2$. In this situation we notice that it is convenient and provides a more transparent picture of the system to perform the following canonical transformation:

$$\begin{bmatrix} c_{1,k,\sigma} \\ c_{2,k,\sigma} \end{bmatrix} = \frac{1}{\sqrt{2}} \begin{bmatrix} e^{+i\pi/4} & e^{-i\pi/4} \\ e^{-i\pi/4} & e^{+i\pi/4} \end{bmatrix} \begin{bmatrix} c_{L,k,\sigma} \\ c_{R,k,\sigma} \end{bmatrix}. \tag{2.7}$$

Under this transformation, the Hamiltonian for the leads Eq. (2.1) is rewritten as follows:

$$\mathcal{H}_0 = \sum_{\mu=1,2}\sum_{k,\sigma} \varepsilon_k c^\dagger_{\mu,k,\sigma} c_{\mu,k,\sigma}, \tag{2.8}$$

while the tunneling Hamiltonian Eq. (2.3) reads

$$\mathcal{H}_T = \sum_{i=1,2}\sum_{\mu=1,2}\sum_{k,\sigma} V_{\mu,i} c^\dagger_{\mu,k,\sigma} d_{i,\sigma} + \text{H.c.}, \tag{2.9}$$

where

$$V_{1,1} = V_{2,2} = \cos\frac{\phi - \pi}{4},$$

$$V_{1,2} = V_{2,1} = \cos\frac{\phi + \pi}{4}. \tag{2.10}$$

Now, the Schrieffer-Wolff transformation[36] of the Hamiltonians Eqs. (2.8), (2.9), and (2.2) leads to the Kondo-type Hamiltonian

$$\begin{aligned} \mathcal{H}_{\text{Kondo}} = \mathcal{H}_0 &+ \tfrac{1}{4}J_1(\mathbf{S}_1 + \mathbf{S}_2)\cdot\left[\psi_1^\dagger(0)\boldsymbol{\sigma}\psi_1(0) + \psi_2^\dagger(0)\boldsymbol{\sigma}\psi_2(0)\right] \\ &+ \tfrac{1}{4}J_2(\mathbf{S}_1 + \mathbf{S}_2)\cdot\left[\psi_1^\dagger(0)\boldsymbol{\sigma}\psi_2(0) + \psi_2^\dagger(0)\boldsymbol{\sigma}\psi_1(0)\right] \\ &+ \tfrac{1}{4}J_3(\mathbf{S}_1 - \mathbf{S}_2)\cdot\left[\psi_1^\dagger(0)\boldsymbol{\sigma}\psi_1(0) - \psi_2^\dagger(0)\boldsymbol{\sigma}\psi_2(0)\right] \\ &- \tfrac{1}{4}J_4\mathbf{S}_1\cdot\mathbf{S}_2. \end{aligned} \tag{2.11}$$

In Eq. (2.11), we have adopted the spinor representations

$$\psi_j = \begin{bmatrix} d_{j,\uparrow} \\ d_{j,\downarrow} \end{bmatrix}, \quad \psi_{\mu,k} = \begin{bmatrix} c_{\mu,k,\uparrow} \\ c_{\mu,k,\downarrow} \end{bmatrix} \tag{2.12}$$

($j = 1,2$ and $\mu = 1,2$), according to which the spin operator on the dot $j$ is given by

$$\frac{\hbar}{2}\mathbf{S}_j = \frac{\hbar}{2}\psi_j^\dagger\boldsymbol{\sigma}\psi_j, \tag{2.13}$$

where $\boldsymbol{\sigma}$ denotes the three Pauli matrices.

The coupling constants $J_i$ ($i = 1, \ldots, 4$) in Eq. (2.11) are given initially (in the RG sense) by

$$J_1 = 2\mathcal{N}\frac{|V|^2}{|\varepsilon_d|}, \quad J_2 = J_1\cos(\phi/2), \quad J_3 = J_1\sin(\phi/2), \tag{2.14}$$

where $\mathcal{N}$ is the spin degeneracy. Under the renormalization group transformation,[37] these coupling constants scale as

$$\frac{dJ_1}{d\ell} = \rho_0(J_1^2 + J_2^2 + J_3^2), \quad \frac{dJ_2}{d\ell} = 2\rho_0 J_1 J_2, \quad \frac{dJ_3}{d\ell} = 2\rho_0 J_1 J_3, \tag{2.15}$$

where $\ell = -\log D$ indicates the renormalization steps ($D$ is the bandwidth). $J_4$ is given by[38–40]

$$J_4 \approx 2\rho_0 J_1^2(0)\Upsilon(D)(1+\cos\phi), \tag{2.16}$$

where $\Upsilon(D)$ is order 1. $J_4$ corresponds to a ferromagnetic RKKY coupling between the spins in the dots.

Under the renormalization group transformation all the system flows to the strong coupling fixed point, with the ratios $J_2/J_1$, $J_3/J_1$, and $J_4/J_1$ remaining constant. In particular, the solution for the initial conditions (2.14) satisfies the simple properties

$$\frac{J_2}{J_1} = \cos(\phi/2), \quad \frac{J_3}{J_1} = \sin(\phi/2), \tag{2.17}$$

with $J_1 \to \infty$ according to the equation

$$\frac{dJ_1}{d\ell} = 2\rho_0 J_1^2. \tag{2.18}$$

From Eq. (2.17) one can easily see that system behaves in distinctive ways for different values of flux $\phi$, especially, for $\phi=0 \pmod{2\pi}$ and $\phi=\pi \pmod{2\pi}$. In the absence of the external flux ($\phi=0$), $J_3=0$ while $J_1=J_2=J$ and $J_4=I=\rho_0 J_1^2/2$. Thus, the Kondo-type Hamiltonian (2.11) is reduced to

$$\mathcal{H}_{\rm Kondo} = \mathcal{H}_0 + \tfrac{1}{4}J(\mathbf{S}_1+\mathbf{S}_2)[\psi_1(0)+\psi_2(0)]^\dagger \boldsymbol{\sigma}[\psi_1(0)+\psi_2(0)] - I\mathbf{S}_1\cdot\mathbf{S}_2. \tag{2.19}$$

This is the two-impurity [characterized by the two spins $(\hbar/2)\mathbf{S}_1$ and $(\hbar/2)\mathbf{S}_2$] Kondo model coupled to a single conduction band (characterized by $\psi_1+\psi_2$, or equivalently $c_{1,k,\sigma}+c_{2,k,\sigma}$). The two spins are coupled to each other ferromagnetically ($-I\mathbf{S}_1\cdot\mathbf{S}_2$, with $I>0$). Due to the ferromagnetic coupling, and to the fact that both spins are coupled to the same conduction band, the total spin is underscreened at $T\to 0$.[38] Note that a strong RKKY interaction may arise from our peculiar geometry since both QDs are directly connected to a single channel in the leads. Nevertheless, in an actual experimental situation[23,29] the QDs are far apart and the RKKY interaction may be negligible. Furthermore, slightly above $\phi=0 \pmod{2\pi}$, even for a *large* ferromagnetic coupling $|I| \gg T_K = D\exp(-1/2\rho_0 J)$, the spins of the dots added in a $S=1$ state become effectively screened.[38]

For the flux $\phi=\pi \pmod{2\pi}$, the coupling constant $J_2=0$ while $J_1=J_3=J_4/2\equiv J$. Then, the Kondo-type Hamiltonian (2.11) is reduced to

$$\mathcal{H}_{\rm Kondo} = \mathcal{H}_0 + \tfrac{1}{2}J\mathbf{S}_1\cdot\psi_1^\dagger(0)\boldsymbol{\sigma}\psi_1(0) + \tfrac{1}{2}J\mathbf{S}_2\cdot\psi_2^\dagger(0)\boldsymbol{\sigma}\psi_2(0) - \tfrac{1}{2}J\mathbf{S}_1\cdot\mathbf{S}_2. \tag{2.20}$$

This model is clearly distinguished from the one in the previous case of $\phi=0 \pmod{2\pi}$ cf. Eq. (2.19). The two impurity spins $(\hbar/2)\mathbf{S}_1$ and $(\hbar/2)\mathbf{S}_2$, of magnitude $1/2$ are coupled to two independent conduction bands, $\psi_1$ and $\psi_2$ (or equivalently $c_{1,k,\sigma}$ and $c_{2,k,\sigma}$), individually. The ferromagnetic coupling in Eq. (2.20) does not play any significant role in this case, because its coupling strength ($I$) is the same as the exchange coupling between the localized spins and the itinerant spins. Therefore, the model (2.20) corresponds to the usual single-channel spin-$1/2$ Kondo model.

The coupling constants scale according to the renormalization group equation

$$\frac{dJ}{d\ell} = 2\rho_0 J^2, \tag{2.21}$$

and the Kondo temperature is given by

$$T_K \sim D\exp\left(-\frac{1}{2\rho_0 J}\right). \tag{2.22}$$

In the general case ($\phi\neq 0,\pi$), the two localized spins $(\hbar/2)\mathbf{S}_1$ and $(\hbar/2)\mathbf{S}_2$ are coupled to two conduction bands $\psi_1$ and $\psi_2$, let alone the ferromagnetic coupling with each other. Unlike the previous, special case of $\phi=\pi$, the two conduction bands are no longer independent; see Eq. (2.11). This fact makes the physical interpretation of the model rather involved. However, the renormalization group flow [see Eqs. (2.17) and (2.18)] and the results from the numerical renormalization group method (see below) suggest that *for any finite flux ($\phi\neq 0$), the two localized spins are fully screened out at zero temperature*.

### *2. Case $U_{12}\to\infty$*

We now investigate the limit of $U_{12}\to\infty$ where the system properties change completely. In this case, only one electron is accommodated in the whole double QD system, i.e., $\langle n_1+n_2\rangle \approx 1$ having either spin ↑ or spin ↓. The orbital degrees of freedom (pseudospin) play as significant a role as the spin, and the double QD behaves as an impurity with four degenerate levels with different tunneling amplitudes depending on the applied flux. Due to the orbital degrees of freedom involved in the interference, the symmetry of the wave function is crucial. Therefore, in this limit, it is more useful to work with a representation in terms of the symmetric (even) and antisymmetric (odd) combinations of the localized and delocalized orbital channels.[11]

In accordance with these observations, we take the following canonical transformations:

$$\begin{bmatrix} d_{e,\sigma} \\ id_{o,\sigma}\end{bmatrix} = \frac{1}{\sqrt{2}}\begin{bmatrix} 1 & 1 \\ 1 & -1\end{bmatrix}\begin{bmatrix} d_{1,\sigma} \\ d_{2,\sigma}\end{bmatrix}, \tag{2.23}$$

for the QD electrons, and

$$\begin{bmatrix} c_{e,k,\sigma} \\ c_{o,k,\sigma}\end{bmatrix} = \frac{1}{\sqrt{2}}\begin{bmatrix} 1 & 1 \\ 1 & -1\end{bmatrix}\begin{bmatrix} c_{L,k,\sigma} \\ c_{R,k,\sigma}\end{bmatrix}, \tag{2.24}$$

for the conduction electrons.

Then, we identify the pseudospin up (down) as the electron occupying the even (odd) orbital. More explicitly, taking the four-spinor representation

$$\psi_d = [d_{e,\uparrow}, d_{e,\downarrow}, d_{o,\uparrow}, d_{o,\downarrow}], \tag{2.25}$$

the spin and orbital pseudo-spin operators are given by

$$\frac{\hbar}{2}\mathbf{S} = \frac{\hbar}{2}\psi_d^\dagger \boldsymbol{\sigma}\psi_d, \quad \frac{\hbar}{2}\overline{\mathbf{T}} = \frac{\hbar}{2}\psi_d^\dagger \boldsymbol{\tau}\psi_d, \tag{2.26}$$

respectively, where $\boldsymbol{\sigma}(\boldsymbol{\tau})$ are Pauli matrices operating on the spin (pseudospin) space. Notice that in this even/odd basis the dot pseudospin has been rotated: $\overline{T}^x \rightarrow T^z$, $\overline{T}^y \rightarrow -T^y$, and $\overline{T}^z \rightarrow T^x$, whereas the spin remains invariant.

In terms of the new operators $d_{e,\sigma}$, $d_{o,\sigma}$, $c_{e,k,\sigma}$, and $c_{o,k,\sigma}$, the total Hamiltonian, $\mathcal{H}_{\text{total}}$ is rewritten as follows:

$$\begin{aligned}\mathcal{H}_D = &\sum_{\alpha=e,o}\sum_{k,\sigma}\varepsilon_{k,\sigma}c_{\alpha,k,\sigma} + \sum_{\alpha=e,o}\Bigg[\sum_{\sigma}\epsilon_d d^\dagger_{\alpha,\sigma}d_{\alpha,\sigma} + \tfrac{1}{2}(U \\ &+ U_{12})n_{\alpha,\uparrow}n_{\alpha,\downarrow}\Bigg] + \tfrac{1}{4}(U+3U_{12})n_e n_o - \tfrac{1}{4}(U-U_{12}) \\ &\times(d_e^\dagger\boldsymbol{\sigma}d_e)\cdot(d_o^\dagger\boldsymbol{\sigma}d_o) - \tfrac{1}{2}(U-U_{12})(d^\dagger_{e,\uparrow}d^\dagger_{e,\downarrow}d_{o,\downarrow}d_{o,\uparrow} \\ &+ \text{H.c.}) + \sum_{\alpha=e,o}\sum_{k,s}V_\alpha c^\dagger_{\alpha,k,s}d_{\alpha,s} + \text{H.c.},\end{aligned} \tag{2.27}$$

where

$$V_e \equiv 2V\cos(\phi/4), \quad V_o \equiv 2V\sin(\phi/4). \tag{2.28}$$

Therefore, the even (odd) orbitals are coupled only to the even(odd)-symmetric combinations of the conduction bands.

To examine the low-energy properties of the system, we obtain for all values of $\phi$ the following effective Hamiltonian by performing a Schrieffer-Wolf transformation:[36]

$$\begin{aligned}\mathcal{H}_{\text{Kondo}} = &\mathcal{H}_0 + \tfrac{1}{4}J_1\mathbf{S}\cdot(\psi^\dagger\boldsymbol{\sigma}\psi) + \tfrac{1}{4}J_2\mathbf{S}\cdot(\psi^\dagger\boldsymbol{\sigma}\overline{\boldsymbol{\tau}}^\perp\psi)\cdot\overline{\mathbf{T}}^\perp \\ &+ \tfrac{1}{4}J_1\mathbf{S}\cdot(\psi^\dagger\boldsymbol{\sigma}\overline{\tau}^z\psi)\overline{T}^2 + \tfrac{1}{4}J_2(\psi^\dagger\overline{\boldsymbol{\tau}}^\perp\psi)\cdot\overline{\mathbf{T}}^\perp \\ &+ \tfrac{1}{4}J_3(\psi^\dagger\overline{\tau}^z\psi)\overline{T}^z + \tfrac{1}{4}J_4[\mathbf{S}\cdot(\psi^\dagger\boldsymbol{\sigma}\overline{\tau}^z\psi) \\ &+ \mathbf{S}\cdot(\psi^\dagger\boldsymbol{\sigma}\psi)\overline{T}^z] - J_5\overline{T}^z,\end{aligned} \tag{2.29}$$

where $\mathcal{H}_0$ is the first term in Eq. (2.27) and $\psi = [\psi_{e\uparrow},\psi_{e\downarrow},\psi_{o\uparrow},\psi_{o\downarrow}]$ is the spinor of the itinerant electrons. Here, the effective coupling constants $J_i$ $(i=1,\ldots,6)$ are initially (in the RG sense) given by

$$J_1 = J_3 = 2\mathcal{N}\frac{|V|^2}{|\varepsilon_d|}, \quad J_2 = J_1\sin(\phi/2), \quad J_4 = J_1\cos(\phi/2), \tag{2.30}$$

and scale according to the RG equations (up to the second order in $J$s)

$$\frac{dJ_1}{d\ell} = 2\rho_0(J_1^2 + J_2^2 + J_4^2), \quad \frac{dJ_2}{d\ell} = \rho_0 J_2(3J_1 + J_3),$$

$$\frac{dJ_3}{d\ell} = 4\rho_0 J_2^2, \quad \frac{dJ_4}{d\ell} = 4\rho_0 J_1 J_4. \tag{2.31}$$

$J_5$ is given and by[38–40]

$$\begin{aligned}J_5 = &4\rho_0|V|^2\cos(\phi/2)\ln\frac{\varepsilon_d + D}{\varepsilon_d - D} \\ &+ 8[\rho_0 J_1(\ell = 0)]^2\Upsilon(D)\cos(\phi/2).\end{aligned} \tag{2.32}$$

As one can see from the RG equations (2.31), in general, each coupling constant in Eq. (2.29) scales differently under the renormalization group transformation for typical behaviors of the solutions at different values of flux $\phi$. Importantly, we show now that the system exhibits a crossover from 0 flux to $\pi$ flux. Near the 0 flux $[\phi \approx 0 \pmod{2\pi}]$, the double-QD odd orbital is completely decoupled from the odd-symmetric lead and only the even orbital is coupled to the even-symmetric conduction lead with $V_e = 2V$ [see Eq. (2.28)]. Equation (2.29) then reduces to a model involving only the spin in the even orbital $(\hbar/2)\mathbf{S}_e$ [not $(\hbar/2)\mathbf{S}$]

$$\mathcal{H}_{\text{Kondo}} = \mathcal{H}_0 + J\mathbf{S}_e\cdot(\psi_e^\dagger\boldsymbol{\sigma}\psi_e)(1+\overline{T}^z) + \tfrac{1}{4}J(\psi_e^\dagger\psi_e)\overline{T}^z - J_5\overline{T}^z, \tag{2.33}$$

where $J = 2|V|^2/|\varepsilon_d|$. This model was already analyzed in Ref. 41, where it was shown that the ground state corresponds to a Fermi liquid state with a greatly enhanced Kondo temperature $T_K^{\text{SU}(2)} = D\exp(-1/4\rho_0 J)$ (due to a coupling doubling of the even orbital to the even-symmetric conduction lead, i.e., $V_e = 2V$) and the orbital pseudospin gets frozen completely, $\overline{T}^z = 1$. ($J_5$ does not flow to the strong coupling regime.) One can easily see that the model (2.33) is equivalent to the two-fold orbitally degenerate Anderson model described by the common *SU(2) Kondo physics*.[33]

Near the $\pi$ flux $[\phi \approx \pi \pmod{2\pi}]$ the exchange couplings are $J = J_1 = J_2 = J_3$, and $J_4 = J_5 = 0$. The corresponding Kondo-type Hamiltonian reads

$$\mathcal{H}_K = \frac{J}{4}[\mathbf{S}\cdot(\psi^\dagger\boldsymbol{\sigma}\psi) + (\psi^\dagger\boldsymbol{\tau}\psi)\cdot\mathbf{T} + \mathbf{S}\cdot(\psi^\dagger\boldsymbol{\sigma}\boldsymbol{\tau}\psi)\cdot\mathbf{T}]. \tag{2.34}$$

This is the celebrated *SU(4) Kondo model*, where the spin and the orbital degrees of freedom become entangled due to the third term in Eq. (2.34). The RG equation reads

$$dJ/d\ell = 4\rho_0 J^2, \tag{2.35}$$

leading to

$$T_K^{\text{SU}(4)} = D\exp(-1/4\rho_0 J). \tag{2.36}$$

As the flux departs from $\pi$, the degeneracy of the even and odd orbitals is lifted and the SU(4) symmetry is broken, much like a single Kondo impurity in the presence of a Zeeman splitting.[42] The crossover from the SU(4) to the SU(2) Kondo model occurs at a given critical flux $\phi_c$. From our NRG calculation (see below) we estimate $\phi_c \approx 0.75\pi$.

This discussion demonstrates the existence of high-symmetry Kondo states in double-quantum systems with interdot interaction in the presence of an Aharonov-Bohm flux. We have shown that the magnetic flux critically alters the properties of the ground state, resulting in a smooth transition from SU(2) to SU(4) Kondo physics. Below, we prove that the *differential conductance* would indicate the principal features of this effect. This is important since it would serve as a means of experimental detection.

### B. Slave-boson mean-field theory

In this section, we adopt the so-called slave-boson mean-field theory which captures the main physics of the Kondo problem[43] at sufficiently low temperatures ($T \ll T_K$). The SBMFT corresponds to the leading order in a $\mathcal{N}$-large expansion, where $\mathcal{N}$ is the degeneracy of each site. Such a SBMFT has been recently applied to study the Kondo effect in nonequilibrium situations[44,45] and in double-QDs systems.[12,13,15]

#### 1. Case $U_{12} \to 0$

First, we consider the case of vanishing interdot Coulomb interaction $U_{12}=0$. We express the two-impurity Anderson model ($\mathcal{H}_{\text{total}}$) in terms of the slave-boson operators. This way the fermionic operator of each dot is written as a combination of a pseudofermion and a boson operator: $d_{i,\sigma}=b_i^\dagger f_{i,\sigma}$, where $f_{i,\sigma}$ is the pseudofermion which annihilates one "occupied state" in the $i$th dot and $b_i^\dagger$ is a boson operator which creates an "empty state" in the $i$th dot. We include two constraints to prevent double occupation in each QD in the limit $U_1, U_2 \to \infty$ by using two Lagrange multipliers $\lambda_1, \lambda_2$. Thus, the Hamiltonian in the slave-boson language reads

$$\begin{aligned}\mathcal{H}_{\text{SB}} &= \mathcal{H}_0 + \sum_{i=1,2}\sum_{\sigma} \varepsilon_{i,\sigma} f_{i,\sigma}^\dagger f_{i,\sigma} \\ &\quad + \frac{1}{\sqrt{\mathcal{N}}}\sum_{i=1,2}\sum_{\ell=L,R}\sum_{k,\sigma}\left(\overline{W}_{\ell,i} c_{\ell,k,\sigma}^\dagger b_i^\dagger f_{i,\sigma} + \text{H.c.}\right) \\ &\quad + \sum_{i=1,2}\lambda_i\left(\sum_\sigma f_{i,\sigma}^\dagger f_{i,\sigma} + b_i^\dagger b_i - 1\right), \end{aligned} \tag{2.37}$$

where $\overline{W}_{\ell,i}=W_{\ell,i}\sqrt{\mathcal{N}}$. The hallmark of the SBMFT consists of replacing the boson operator by its classical (nonfluctuating) average. $b_i(t)/\sqrt{\mathcal{N}} \to \langle b_i\rangle/\sqrt{\mathcal{N}} \equiv \widetilde{b}_i$, thereby neglecting charge fluctuations in each dot. This approximation is exact in the limit $\mathcal{N}\to\infty$, and it corresponds to $\mathcal{O}(1)$ in a $1/\mathcal{N}$ expansion. At zero temperature $T=0$, it correctly describes spin fluctuations (Kondo regime). Then, the mean-field Hamiltonian is given by

$$\begin{aligned}\mathcal{H}_{\text{MF}} &= \mathcal{H}_0 + \sum_i\sum_\sigma \widetilde{\varepsilon}_{i,\sigma} f_{i,\sigma}^\dagger f_{i,\sigma} + \sum_i \sum_{\ell,k,\sigma}\left(\widetilde{W}_{\ell,i} c_{\ell,k,\sigma}^\dagger f_{i,\sigma} + \text{H.c.}\right) \\ &\quad + \sum_i \lambda_i\left(\mathcal{N}|\widetilde{b}_i|^2 - 1\right), \end{aligned} \tag{2.38}$$

where $\widetilde{W}_{\ell,i}=\widetilde{b}_i\overline{W}_{\ell,i}$. We obtain a quadratic Hamiltonian containing four parameters ($\widetilde{b}_{1,2}$ and renormalized levels $\widetilde{\varepsilon}_{1,2}=\varepsilon_d+\lambda_{1,2}$) to be determined from mean-field equations.[13,43] These mean-field equations are the constraints for the dot $i=1,2$

$$\sum_\sigma \langle f_{i,\sigma}^\dagger(t) f_{i,\sigma}(t)\rangle + \mathcal{N}|\widetilde{b}_i|^2 = 1, \tag{2.39}$$

and the equations of motion (EOM) of the boson fields

$$\sum_{\ell,k,\sigma}\widetilde{W}_{\ell,i}\left\langle c_{k,\sigma}^\dagger(t) f_{i,\sigma}(t)\right\rangle + \lambda_i \mathcal{N}|\widetilde{b}_i|^2 = 0. \tag{2.40}$$

The next step is to write these mean-field equations in terms of nonequilibrium Green functions. The lesser dot-dot Green function is $(i\in 1,2) G_{i,\sigma}^<(t-t')=-i\langle f_{i,\sigma}^\dagger(t') f_{i,\sigma}(t)\rangle$, and the corresponding lesser lead-dot Green function is $G_{i,\sigma;\ell,k,\sigma}^<(t-t')=-i\langle c_{\ell,k,\sigma}^\dagger(t') f_{i,\sigma}(t)\rangle$. By applying the equation-of-motion (EOM) technique and the analytical continuation rules[46,47] we can relate the lesser lead-dot Green function with the dot-dot Green function. Eventually, the explicit form of the Green's functions can be found easily using the EOM technique. This way, we close the set of mean-field equations, which are self-consistently solved for each set of parameters (the dot levels $\varepsilon_i$, the tunneling amplitudes $V_{\ell,i}$, the flux $\phi$, the bandwidth $D$, and the applied dc bias $V_{\text{dc}}$).

At zero bias we can derive analytical expressions of $T_K$ ($\phi$-dependent) within the SBMFT. For example, for $\pi$-flux we get $T_K^{\text{SU}(2)}=D\exp(-\pi|\varepsilon_d|/2\Gamma)$ ($\Gamma=\pi\rho_0|V|^2$ is the hybridization width). As expected, it is in agreement with scaling theory, see Eq. (2.22).

#### 2. Case $U_{12} \to \infty$

For $U_{12}\to\infty$ only one dot can be charged at a given time. In this case we introduce one boson field and one constraint that preserves the condition $\langle n_1+n_2\rangle=1$. The rest of the calculation follows the lines exposed above. We find for the Kondo temperature at $\phi=\pi$ $T_K^{\text{SU}(4)}=(D/\sqrt{2})\exp(-\pi|\varepsilon_d|/4\Gamma)$ [cf. Eq. (2.36)].

#### 3. Transport properties

We next describe how to calculate the current through the double-QD system within the SBMFT. The simplicity of our approach allows us to write the current using the Landauer-Büttiker formula

$$I = \frac{2e}{\hbar}\int \frac{d\varepsilon}{2\pi}\mathcal{T}(\varepsilon, V_{\text{dc}})[f_L(\varepsilon) - f_R(\varepsilon)], \tag{2.41}$$

where $\mathcal{T}(\varepsilon, V_{\text{dc}})$ is the transmission probability which depends on renormalized parameters. Following Meir and Wingreen,[48] the transmission through this system can be obtained using

$$\mathcal{T} = \text{Tr}\{\hat{G}^a\widetilde{\Gamma}_R\hat{G}^r\widetilde{\Gamma}_L\}. \tag{2.42}$$

Here, $\hat{G}^{a(r)}$ is the matrix of the advanced (retarded) Green's function for the dot electrons; i.e., $G_{i,j;\sigma}^{r/a}(t)=\mp i\theta(\pm t)\times\langle\{d_{i,\sigma}(t), d_{j,\sigma}^\dagger(0)\}\rangle$. $\widetilde{\Gamma}_\ell$ is the matrix of the renormalized hybridization parameters; i.e., $\widetilde{\Gamma}_{\ell;i,j}=\pi\rho_\ell\overline{W}_{\ell,i}\overline{W}_{\ell,j}^*\widetilde{b}_i\widetilde{b}_j^*$ for $U_{12}=0$ and $\widetilde{\Gamma}_{\ell;i,j}=\pi\rho_\ell\overline{W}_{\ell,i}\overline{W}_{\ell,j}^*|\widetilde{b}|^2$ for $U_{12}=\infty$.

For identical dots and symmetric junctions, the transmission probability is given by

$$\mathcal{T}(\epsilon) = \frac{\widetilde{\Gamma}^2\left[(\epsilon-\widetilde{\varepsilon}_d)^2\cos^2\dfrac{\phi}{2}\right]}{\left[(\epsilon-\widetilde{\varepsilon}_d)^2 - \left(\dfrac{\widetilde{\Gamma}}{2}\right)^2\sin^2\dfrac{\phi}{2}\right]^2 + (\epsilon-\widetilde{\varepsilon}_d)^2\widetilde{\Gamma}^2}, \tag{2.43}$$

regardless of whether $U_{12}=0$ or $U_{12}=\infty$. Of course, the renormalized coupling $\widetilde{\Gamma}$ in the above equation should be obtained according to the different set of mean-field equations, depending on whether $U_{12}=0$ or $U_{12}=\infty$. We notice that Eq. (2.43) was previously obtained in Refs. 30 and 31 for the noninteracting case.

The expression for the nonlinear conductance is straightforward from the current expression $I$: $\mathcal{G}=dI/dV_{dc}$. In the same way, the linear conductance $\mathcal{G}_0$ is determined upon insertion of the total transmission evaluated at the Fermi energy into the well-known formula

$$\mathcal{G}_0 = \frac{2e^2}{h}\mathcal{T}(E_F). \tag{2.44}$$

### C. Numerical renormalization group

SBMFT does not take fully into account real charge fluctuation effects. In order to confirm our previous results and make quantitative predictions, we also use the NRG procedure.[49–52]

Following the standard NRG procedures,[49–51] we evaluate the various physical quantities from the recursion relation ($N\geqslant 0$)

$$\tilde{\mathcal{H}}_{N+1} = \sqrt{\Lambda}\tilde{\mathcal{H}}_N + \xi_{N+1}\sum_{\mu=e,o}\sum_{\sigma=\uparrow\downarrow}\left(f^\dagger_{\mu,N,\sigma}f_{\mu,N+1,\sigma} + \text{H.c.}\right), \tag{2.45}$$

with the initial Hamiltonian given by

$$\tilde{\mathcal{H}}_0 = \frac{1}{\sqrt{\Lambda}}\left[\tilde{\mathcal{H}}_D + \sum_{\mu=e,o}\sum_{\sigma}\tilde{V}_\mu(d^\dagger_\sigma f_{\mu,0,\sigma} + \text{H.c.})\right]. \tag{2.46}$$

Here, the fermion operators $f_{\mu,N,\sigma}$ have been introduced as a result of the logarithmic discretization, and the accompanying canonical transformation, $\Lambda$, is the logarithmic discretization parameter (we choose $\Lambda=2$)

$$\xi_N \equiv \frac{1-\Lambda^{-N}}{\sqrt{[1-\Lambda^{-(2N-1)}][1-\Lambda^{-(2N+1)}]}}, \tag{2.47}$$

and

$$\tilde{\mathcal{H}}_D \equiv \zeta\frac{\mathcal{H}_D}{D}, \tag{2.48}$$

with $\zeta=2/(1+1/\Lambda)$. The coupling constants $\tilde{V}_e$ and $\tilde{V}_o$, respectively, are given by

$$\tilde{V}_e \equiv 4\zeta\sqrt{\frac{2\Gamma}{\pi D}}\cos(\phi/4), \tag{2.49}$$

$$\tilde{V}_o \equiv 4\zeta\sqrt{\frac{2\Gamma}{\pi D}}\sin(\phi/4). \tag{2.50}$$

The Hamiltonians $\tilde{\mathcal{H}}_N$ in Eq. (2.45) have been rescaled for numerical accuracy. The original Hamiltonian is recovered by

$$\frac{\mathcal{H}}{D} = \lim_{N\to\infty}\frac{\tilde{\mathcal{H}}_N}{\mathcal{S}_N}, \tag{2.51}$$

with $\mathcal{S}_N\equiv\zeta\Lambda^{(N-1)/2}$.

In the following, we study the local Green's functions (with which the linear conductance is calculated) and the dynamic spin susceptibility. To improve accuracy at higher energies, we adopt the density-matrix NRG method (DM-NRG).[52] In this method, first usual NRG iterations are performed down to the energy scale $\omega_N\equiv D\Lambda^{-N/2}\ll T_K$. From the excitation spectrum at this scale, the density matrix is constructed

$$\rho = \sum_m e^{-E^N_m/\omega_N}|m\rangle_N\langle m|, \tag{2.52}$$

where $|m\rangle_N$ is the the eigenstate of $\mathcal{H}_N$ with energy $E^N_m$. Then, the NRG iterations are performed again, but now at each iteration $N'$, calculating the Green's function by

$$G_{\mu\sigma;\mu'\sigma'}(t) = \frac{i}{\hbar}\theta(t)\text{Tr}\,\rho_{N'}[d_{\mu,\sigma}(t),d^\dagger_{\mu',\sigma'}], \tag{2.53}$$

where

$$\rho_{N'} \equiv \text{Tr}_{N>N'}\rho \tag{2.54}$$

is the reduced density matrix for the cluster of size $N'$. The Green's function in Eq. (2.53) is valid at the frequency scale $\omega\simeq\omega_{N'}$. The spin susceptibility is calculated in the same manner

$$\chi(\omega) = -\frac{1}{\pi}\text{Im}\int_{-\infty}^{\infty}dte^{+i\omega t}\frac{1}{i\hbar}\text{Tr}\,\rho_{N'}\{s_z(t),s_z\}, \tag{2.55}$$

where

$$s_z \equiv \tfrac{1}{2}\sum_\mu[d^\dagger_{\mu,\uparrow}d_{\mu,\uparrow} - d^\dagger_{\mu,\downarrow}d_{\mu,\downarrow}]. \tag{2.56}$$

## III. NUMERICAL RESULTS

We now present our results for the electronic transport in both limits of the Coulomb interaction, $U_{12}\to 0$ and $U_{12}\to\infty$. In the numerical calculations, the model parameters are taken as follows: symmetric couplings ($\Gamma_{1(2)L}=\Gamma_{1(2)R}=\Gamma/2$) and equal level positions ($\varepsilon_1=\varepsilon_2=\varepsilon_d$). Throughout this paper, all the parameters are given in units of the bare coupling $\Gamma$. The energy cutoff is set as $D=60\Gamma$.

### A. Case $U_{12}\to 0$

In the left panel of Fig. 2, we present our results when $U_{12}\to 0$ obtained with slave-boson mean-field theory. First, we focus on the pure Kondo regime when $\varepsilon_d=-3.5$ and discuss both the linear conductance and the nonlinear conductance [given by $\mathcal{G}_0\equiv\mathcal{G}(V_{dc}=0)$ and $\mathcal{G}\equiv dI/dV_{dc}$, respectively]. The linear conductance [solid line in Fig. 2(a)] shows *narrow* peaks due to constructive interference around $\phi\approx 0 \pmod{2\pi}$, whereas transport is suppressed elsewhere. This is due to the fact that the DOS of each dot has a resonance exactly at $E_F$. In the language of slave bosons this means $\tilde{\varepsilon}_{1,2}=0$ and a SU(2) Kondo state is well formed. Therefore, these narrow peaks in $\mathcal{G}_0$ correspond to paths through the AB geometry with multiple windings around the enclosed flux. The width of each peak is given roughly by $\approx T_K$. Away from the constructive interference condition, the

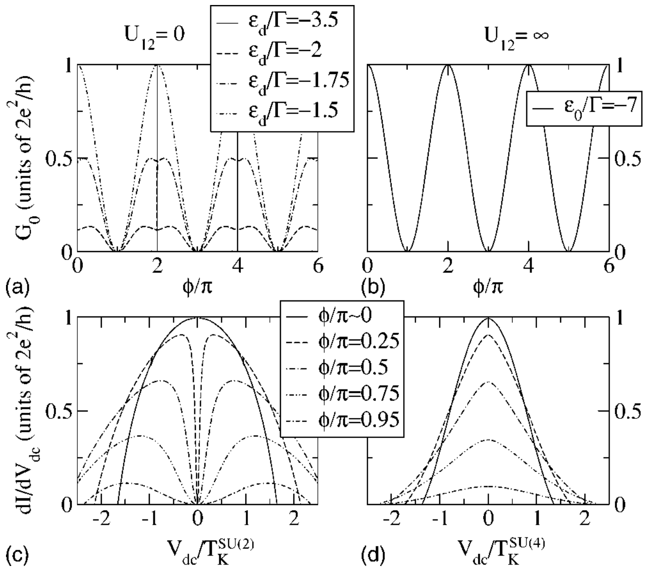


FIG. 2. *SBMFT results:* Left panel ($U_{12}\to 0$): (a) Linear conductance ($\mathcal{G}_0$) versus flux $\phi$ for different level positions. When the Kondo state is formed (for $\varepsilon_d=-3.5$) the $\mathcal{G}_0$ are delta-like peaks of height 1 centered at even multiples of $\phi/\pi$. (c) Curves for $\mathcal{G}$ versus voltage bias for $\varepsilon_d=-3.5$. Here, we change the flux from 0 (full line) to $\pi$ (dot-dot-dashed line). Right panel ($U_{12}\to\infty$): (b) linear and (d) differential conductance. Energies are measured in units of $\Gamma=\pi\rho_0|V|^2=D/60$.

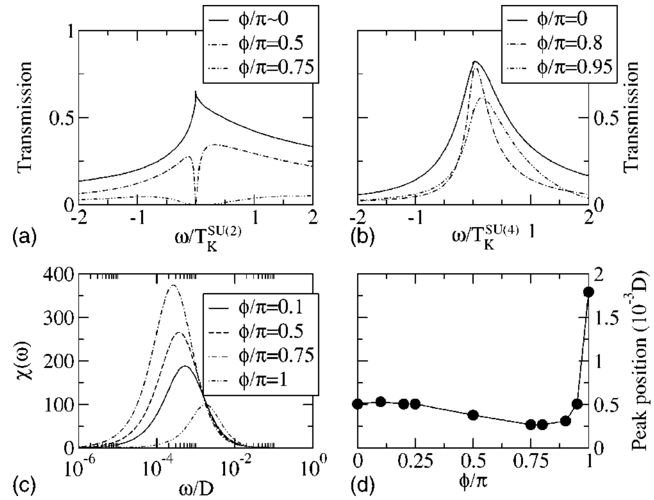


FIG. 3. *NRG results:* Top panel: Transmission probability versus flux for (a) $\varepsilon_d=-7\Gamma$, $U_1=U_2=5D$, $U_{12}=0$, and (b) $\varepsilon_d=-14\Gamma$, $U_1=U_2=5D$, and $U_{12}=5D$. We set $\Gamma=D/60$. [Notice that we do not recover the unitary limit of $\mathcal{T}$ for $\phi\approx 0 \pmod{2\pi}$ because of the systematic errors introduced in the NRG procedure]. Bottom panel ($U_{12}=5D$): (c) Spin susceptibility (in an arbitrary unit) in the limit of strong interdot interaction. (d) The peak position of the susceptibility as a function of the flux $\phi$.

transmission at the Fermi energy quickly vanishes. This unusual behavior is clarified with our calculations of the differential conductance. In Fig. 2(c) we show the nonlinear conductance $dI/dV_{dc}$ as a function of the bias voltage $V_{dc}$ for different values of the flux and $\varepsilon_d=-3.5$. In the absence of flux (or for even multiples of it) the nonlinear conductance shows the usual zero-bias anomaly (ZBA), a narrow peak at $V_{dc}=0$ that reaches the unitary limit due to the constructive interference in the resonant condition. Increasing $\phi$ does not affect the Kondo resonance much, so the transmission probability $\mathcal{T}$ can be written as a combination of a Breit-Wigner resonance for $\tilde{\varepsilon}_d=0$ plus a Fano antiresonance.[30] A *dip* at zero bias is then obtained [see Fig. 2(c)].[30,32] The width of this dip is $T_K(\phi)[1-\cos(2\phi)]$. It has an oscillatory dependence on the applied flux. This result is in good agreement with the NRG calculations as shown in Fig. 3(a). Here, we plot $\mathcal{T}$ as a function of energy. It is worthwhile to note that $\mathcal{T}$ amounts to $\mathcal{G}$ at low bias.

For increasing $\varepsilon_d$ one enters the mixed-valence regime [see Fig. 2(a)]. Although the results should be taken in a qualitative way, we find that the renormalized levels for $\varepsilon_d=-2$, $-1.75$, $-1.5$ are no longer at $E_F$ except when $\phi\approx 0 \pmod{2\pi}$. The transmission coefficient (and thereby the conductance) is extremely sensitive to deviations of $\tilde{\varepsilon}_d$ out of $E_F$. When the bare level position is shifted toward the Fermi energy the renormalized levels for $\varepsilon_d=-2$, $-1.75$ as a function of $\phi$ are not at $E_F$ except when $\phi\approx 0 \pmod{2\pi}$, whereas for $\varepsilon_d=-1.5$ they never reach $E_F$. In these cases, due to the lack of a resonant condition at each dot, multiple windings are less likely to occur and the conductance starts to resemble a cosine-like function generated by a combination of lower harmonics [see Fig. 2(a), case $\varepsilon_d=-1.5$]. For $\varepsilon_d=-2$, $-1.75$ we still observe the sharp resonance at $\mathcal{G}(\phi\approx 0) \pmod{2\pi}$ due to a quasiresonant condition when $\phi\approx 0 \pmod{2\pi}$. Finally, for $\varepsilon_d=-1.5$ the linear conductance has a trivial cosine dependence.

### B. Case $U_{12}\to\infty$

Next, we elaborate on the numerical results for the limit of a strong interdot Coulomb interaction $U_{12}\to\infty$ (right panel of Fig. 2). The results show that in this situation not only the spin fluctuates but also the pseudospin since just two charge states are allowed in the double-QD system: $\{n_1=1,n_2=0\}$ and $\{n_1=0,n_2=1\}$. The fluctuations in both sectors (spin and pseudospin) lead to the exotic SU(4) state close to $\phi=\pi \pmod{2\pi}$.

We begin with the linear regime. Figure 2(b) summarizes our results for $\mathcal{G}_0$ as a function of the applied flux. We concentrate on the pure Kondo regime and set $\varepsilon_d=-7$, well below $E_F$. Unlike the case of weak interdot Coulomb interaction [see Fig. 2(a)], the linear conductance shows *broad* peaks at positions $\phi\approx 0 \pmod{2\pi}$. In addition, the linear conductance only vanishes when the condition of destructive interference takes place. Let us investigate in some detail the two limit cases $\phi\approx 0$ and $\phi\approx\pi \pmod{2\pi}$. In our RG analysis, we find for $\phi\approx 0 \pmod{2\pi}$ that the ground state corresponds to the usual spin SU(2) Kondo effect with a greatly enhanced Kondo scale. Accordingly, the corresponding renormalized level lies at $\tilde{\varepsilon}_d=0$, leading to a shift of the scattering phase $\delta=\pi/2$. On the contrary, for $\phi=\pi \pmod{2\pi}$ we find that the ground state is the highly symmetric SU(4) Kondo state with a renormalized level at $\tilde{\varepsilon}_d\approx T_K^{SU(4)}$, which implies $\delta=\pi/4$ to fulfill the Friedel-

Langreth sum rule.[4] Quite generally, in a SU($N$) problem the phase shift becomes $\delta=\pi/\mathcal{N}$ in the limit of large $\mathcal{N}$ and the Kondo resonance shifts up to $\tilde{\varepsilon}_d\approx\pi\tilde{\Gamma}/\mathcal{N}$.[4] In the intermediate regime, when $0\lesssim\phi\lesssim\pi$, the renormalized level takes on a positive value $\tilde{\varepsilon}_d<T_K^{\mathrm{SU}(4)}$. As a consequence, away from $\phi\approx 0 \pmod{2\pi}$ the resonant condition is not satisfied (the renormalized level $\tilde{\varepsilon}_d$ is not longer at $E_F$). In this situation electronic paths with multiple windings do not occur and the linear conductance consists of a cosine-like function [Fig. 2(b)]. At finite $V_{\mathrm{dc}}$ the nonlinear conductance displays a ZBA which is quenched as $\phi$ decreases [see Fig. 2(d)], unlike the dip found in the $U_{12}=0$ case. Eventually, for $\phi=\pi \pmod{2\pi}$ there is no transport due to completely destructive interference.

We can compare our results shown in Fig. 2(d) with those obtained from NRG plotted in Fig. 3(b). Here, one can see that $\mathcal{T}$ decreases as $\phi$ increases, which is consistent with the results of the SBMFT. Nevertheless, SBMFT overestimates the decreasing rate of the ZBA. The NRG results show that while the peak does not change appreciably for $\phi<\phi_c$, it decreases very rapidly for $\phi>\phi_c$.

### C. Crossover

The value of $\phi_c$ is the last component we have to explain. $\phi_c$ marks the crossover between SU(2) Kondo physics to the highly symmetric SU(4) Kondo state. Fortunately, $\phi_c$ can be extracted from the peak position of the spin susceptibility $\chi(\omega)$, which yields a reasonable estimate of the Kondo temperature. Figure 3(c) shows the evolution of $\chi$ when $\phi$ increases. Remarkably, when the flux enhances, at some point the position of the peak moves toward higher frequencies. The peak position as a function of $\phi$ is plotted in Fig. 3(d). We observe that $T_K(\phi)$ is almost constant when $\phi$ goes from zero to $\phi_c\approx 0.75\pi$. This fact allows us to establish a criterion for the crossover between the SU(2) and SU(4) Kondo states in the double-QD system.

## IV. CONCLUSION

We have analyzed the transport properties (in and out of equilibrium) of a prototypical mesoscopic double-slit interferometer when interactions play a dominant role. We have shown that crucial differences arise in the limits of negligible and large interdot Coulomb interactions. In the former case, only spin fluctuations matter and each dot develops a Kondo resonance at the Fermi level independently of the applied magnetic flux. Due to the interference between these two Kondo resonances, the linear conductance versus the flux shows a series of narrow peaks at $\phi=2\pi \pmod{2\pi}$ of unitary height (in units of $2e^2/h$). Furthermore, we have found that any deviation from the Kondo regime (close to the mixed-valence regime) leads to dramatic changes in the conductance as a function of the flux. Interestingly, the nonlinear conductance shows the formation of a dip when $\phi\neq 2\pi \pmod{2\pi}$. A complete suppression of the electronic transport occurs when the destructive interference condition takes place, $\phi=\pi \pmod{2\pi}$.

Charge and spin become entangled when the interdot Coulomb interaction is very large. Here, the differential conductance has a zero-bias anomaly quenched with increasing flux. The Kondo state changes its symmetry, from SU(2) to SU(4), as $\phi$ approaches $\pi \pmod{2\pi}$. Since the crossover is not too close to $\phi=\pi \pmod{2\pi}$, the SU(4) state remains robust to be detected experimentally. Our geometry requires symmetric couplings to the leads but not inevitably equal (i.e., we need $V_{L1}+V_{R2}=V_{R1}+V_{L2}$).[53] The charging energies $U_1$, $U_2$, and $U_{12}$ should be of the same order (a few meV). Finally, the external flux should correspond to a low magnetic field to avoid spin Zeeman splittings in the dot, around 10 mT.[29] All these constraints are experimentally accessible with present techniques.[22,23,29]

## ACKNOWLEDGMENTS

This work was supported by the EU RTN No. HPRN-CT-2000-00144, Nanoscale Dynamics, the Spanish MECD, the "Ramón y Cajal" program, the NSERC, the eSSC at Postech, the SKORE-A. and the SK-Fund. K.L.H. thanks CIAR, FQRNT, and NSERC for support.

[1] For a review, see L. P. Kouwenhoven, C. M. Marcus, P. L. McEuen, S. Tarucha, R. M. Westervelt, and N. S. Wingreen, in *Proceedings of the NATO Advanced Study Institute on Mesoscopic Electron Transport*, edited by L. L. Sohn, L. P. Kouwenhoven, and G. Schön, Kluwer Series E345 (Kluwer, Dordrecht, 1997), pp. 105–214.

[2] L. I. Glazman and M. E. Raikh, Pis'ma Zh. Eksp. Teor. Fiz. **47**, 378 (1988) [JETP Lett. **47**, 452 (1988)].

[3] T. K. Ng and P. A. Lee, Phys. Rev. Lett. **61**, 1768 (1988).

[4] A. C. Hewson, *The Kondo Problem to Heavy Fermions* (Cambridge University Press, Cambridge, UK, 1993).

[5] D. Goldhaber-Gordon, H. Shtrikman, D. Mahalu, D. Abusch-Magder, U. Meirav, and M. A. Kastner, Nature (London) **391**, 156 (1998).

[6] S. M. Cronenwett, T. H. Oosterkamp, and L. P. Kouwenhoven, Science **281**, 540 (1998).

[7] J. Schmid, J. Weis, K. Eberl, and K. von Klitzing, Physica B **256–258**, 182 (1998).

[8] S. Hershfield, J. H. Davies, and J. W. Wilkins, Phys. Rev. Lett. **67**, 3720 (1991); Phys. Rev. B **46**, 7046 (1992); Y. Meir, N. S. Wingreen and P. A. Lee, Phys. Rev. Lett. **70**, 2601 (1993); A. L. Yeyati, A. Martín-Rodero, and F. Flores, *ibid.* **71**, 2991 (1993); N. S. Wingreen and Y. Meir, Phys. Rev. B **49**, 11040 (1994); J. König, J. Schmid, H. Schoeller, and G. Schön, *ibid.* **54**, 16820 (1996).

[9] M. H. Hettler and H. Schoeller, Phys. Rev. Lett. **74**, 4907 (1995); T. K. Ng, *ibid.* **76**, 487 (1996); A. Schiller and S. Hershfield, *ibid.* **77**, 1821 (1996); R. López, R. Aguado, G. Platero, and C. Tejedor, *ibid.* **81**, 4688 (1998); Phys. Rev. B **64**, 075319 (2001); Y. Goldin and Y. Avishai, Phys. Rev. Lett. **81**, 5394 (1998); A.

Kaminski, Yu. V. Nazarov, and L. I. Glazman, *ibid.* **83**, 384 (1999); Phys. Rev. B **62**, 8154 (2000); P. Nordlander, N. S. Wingreen, Y. Meir, and D. C. Langreth, *ibid.* **61**, 2146 (2000).

[10] M. Plihal, D. C. Langreth, and P. Nordlander, Phys. Rev. B **61**, R13341 (2000); A. Schiller and S. Hershfield, *ibid.* **62**, R16271 (2000); P. Coleman, C. Hooley, Y. Avishai, Y. Goldin, and A. F. Ho, J. Phys.: Condens. Matter **14**, 205 (2002).

[11] W. Izumida, O. Sakai, and Y. Shimizu, J. Phys. Soc. Jpn. **66**, 717 (1997).

[12] A. Georges and Y. Meir, Phys. Rev. Lett. **82**, 3508 (1999).

[13] R. Aguado and D. C. Langreth, Phys. Rev. Lett. **85**, 1946 (2000); Phys. Rev. B **67**, 245307 (2003).

[14] T. Aono and M. Eto, Phys. Rev. B **63**, 125327 (2001).

[15] R. Lopez, R. Aguado, and G. Platero, Phys. Rev. Lett. **89**, 136802 (2002).

[16] P. Simon, R. López, and Y. Oreg, cond-mat/0404540, Phys. Rev. Lett. (to be published).

[17] H. Jeong, A. M. Chang, and M. R. Melloch, Science **293**, 2221 (2001).

[18] J. C. Chen, A. M. Chang, and M. R. Melloch, Phys. Rev. Lett. **92**, 176801 (2004).

[19] N. J. Craig, J. M. Taylor, E. A. Lester, C. M. Marcus, M. P. Hanson, and A. C. Gossard, Science **304**, 565 (2004).

[20] D. Loss and E. V. Sukhorukov, Phys. Rev. Lett. **84**, 1035 (2000).

[21] For a recent review see W. G. van der Wiel, S. De Franceschi, J. M. Elzerman, T. Fujisawa, S. Tarucha, and L. P. Kouwenhoven, Rev. Mod. Phys. **75**, 1 (2003).

[22] U. Wilhelm and J. Weis, Physica E (Amsterdam) **6**, 668 (2000).

[23] A. W. Holleitner, A. Chudnovskiy, D. Pfannkuche, K. Eberl, and R. H. Blick, Phys. Rev. B **70**, 075204 (2004).

[24] T. Pohjola, H. Schoeller, and G. Schön, Europhys. Lett. **54**, 241 (2001).

[25] L. Borda, G. Zaránd, W. Hofstetter, B. I. Halperin, and J. von Delft, Phys. Rev. Lett. **90**, 026602 (2003).

[26] K. Le Hur and P. Simon, Phys. Rev. B **67**, 201308 (2003).

[27] K. Le Hur, P. Simon, and L. Borda, Phys. Rev. B **69**, 045326 (2004).

[28] Y. Aharonov and D. Bohm, Phys. Rev. **115**, 485 (1959).

[29] A. W. Holleitner, C. R. Decker, H. Qin, K. Eberl, and R. H. Blicket, Phys. Rev. Lett. **87**, 256802 (2001).

[30] T. V. Shahbazyan and M. E. Raikh, Phys. Rev. B **49**, 17 123 (1994).

[31] B. Kubala and J. König, Phys. Rev. B **65**, 245301 (2002).

[32] K. Kang and S. Y. Cho, J. Phys.: Condens. Matter **16**, 117 (2004).

[33] D. Boese, W. Hofstetter, and H. Schoeller, Phys. Rev. B **66**, 125315 (2002).

[34] In particular, the SU(4) Kondo state is known to be robust against small deviations from the perfectly symmetric situation (Ref. 25).

[35] The opposite limit at high $T$ has been recently treated by Y. Utsumi *et al.*, Phys. Rev. B **69**, 155320 (2004).

[36] J. R. Schrieffer and P. A. Wolff, Phys. Rev. **149**, 491 (1966).

[37] P. W. Anderson, J. Phys. C **3**, 2436 (1970).

[38] C. Jayaprakash, H. R. Krishna-murthy, and J. W. Wilkins, Phys. Rev. Lett. **47**, 737 (1981).

[39] I. Affleck, A. W. W. Ludwig, and B. A. Jones, Phys. Rev. B **52**, 9528 (1995).

[40] B. A. Jones and C. M. Varma, Phys. Rev. B **40**, 324 (1989).

[41] G. Zaránd, Phys. Rev. B **52**, 13459 (1995).

[42] In a realistic system, the $J_5$ term of Eq. (2.29) is much smaller than $T_K^{SU(4)}$, preserving the SU(4) state.

[43] P. Coleman, Phys. Rev. B **29**, 3035 (1984). For a review, see D. M. Newns and N. Read, Adv. Phys. **36**, 799 (1987).

[44] B. Dong and X. L. Lei, J. Phys.: Condens. Matter **14**, 4963 (2002).

[45] Y. Avishai, A. Golub, and A. D. Zaikin, Phys. Rev. B **67**, 041301 (2003).

[46] D. C. Langreth, in *Linear and Nonlinear Electron Transport in Solids*, edited by J. T. Devreese and V. E. Van Doren, Nato ASI, Series B, Vol. 17 (Plenum, New York, 1976).

[47] Y. Meir and N. S. Wingreen, Phys. Rev. Lett. **70**, 2601 (1993).

[48] Y. Meir and N. S. Wingreen, Phys. Rev. Lett. **68**, 2512 (1992).

[49] K. G. Wilson, Rev. Mod. Phys. **47**, 773 (1975).

[50] H. R. Krishna-murthy, J. W. Wilkins, and K. G. Wilson, Phys. Rev. B **21**, 1003 (1980).

[51] T. A. Costi, A. C. Hewson, and V. Zlatic, J. Phys.: Condens. Matter **6**, 2519 (1994).

[52] W. Hofstetter, Phys. Rev. Lett. **85**, 1508 (2000).

[53] Any deviation symmetry of the exchange couplings in Eq. (2.34) introduces also a Zeeman term in the pseudospin sect or $\delta E T_z$, where $\delta E$ is the renormalized energy difference between the two charged states $(n_1=0, n_2=1)$ and $(n_1=1, n_2=0)$. Since $T_z$ is a marginal operator at the SU(4) fixed point [see J. Ye, Phys. Rev. B **56**, R489 (1997)] the SU(4) state is robust whenever $\delta E < T_K^{SU(4)}$ (Ref. 25).